RSC Advances

PAPER

View Article Online
View Journal | View Issue



Cite this: *RSC Adv.*, 2017, **7**, 47619

# $WO_3/BiVO_4$ photoanode coated with mesoporous $Al_2O_3$ layer for oxidative production of hydrogen peroxide from water with high selectivity†

Kojiro Fuku,*[a] Yuta Miyase,[ab] Yugo Miseki,[a] Takahiro Gunji[ab] and Kazuhiro Sayama*[ab]

Received 31st August 2017
Accepted 3rd October 2017

DOI: 10.1039/c7ra09693c

rsc.li/rsc-advances

A $WO_3/BiVO_4$ photoanode coated with various metal oxides demonstrated high selectivity (faradaic efficiency) for hydrogen peroxide ($H_2O_2$) generation from water ($H_2O$) under irradiation of simulated solar light in a highly concentrated hydrogen carbonate ($KHCO_3$) aqueous solution. A mesoporous and amorphous aluminium oxide ($Al_2O_3$) layer significantly facilitated inhibition of the oxidative degradation of generated $H_2O_2$ into oxygen ($O_2$) on the photoanode, resulting in unprecedented $H_2O_2$ selectivity (*ca.* 80%) and the accumulation (>2500 μM at 50C).



Chemical conversions using light energy have been performed in various fields since the discovery of the Honda–Fujishima effect.[1–25] Significant efforts have recently been devoted to $H_2$ production by water splitting using inexhaustible light for clean energy conversion processes.[1–4,8–29] Photoelectrode systems are widely recognised as a promising technology for $H_2$ production because they operate at an electrolysis voltage lower than the theoretical electrolysis voltage of water (<1.23 V).[1,8–29] Visible light-responsive oxide photoanodes with a narrow bandgap energy, such as $WO_3$, $BiVO_4$ and $Fe_2O_3$, are desirable for the efficient utilisation of solar light and economical synthetic processes.[8–29] Most importantly, numerous efforts have been focused on $BiVO_4$ photoanodes capable of utilising a wide range of light energy (~520 nm) and achieving efficient $O_2$ generation by water splitting.[9–21,28,29,32] A $WO_3/BiVO_4$ photoanode that combines $BiVO_4$ with a $WO_3$ underlayer for the efficient transfer of excited electrons on $BiVO_4$ to the F-doped $SnO_2$ conductive glass (FTO) substrate shows exceptional photoelectrochemical performance for water splitting into $H_2$ and $O_2$.[10–13,17–20,28,29,32] However, most previous investigations, containing electrochemical reactions, focused solely on the recovery of $H_2$ energy generated on the cathode and little attention was paid to the recovery of the oxidation products simultaneously evolved during water splitting.[24–31]

$H_2O_2$ is an especially versatile and clean oxidation product having the potential to generate instead of $O_2$ from $H_2O$ (eqn (1)).

$$2H_2O \rightarrow H_2O_2 + 2H^+ + 2e^- \ (E(H_2O_2/H_2O) = +1.77 \text{ V } \textit{vs.} \text{ RHE}) \quad (1)$$

However, the accumulation of $H_2O_2$, generated oxidatively is extremely difficult because degradation of $H_2O_2$ into $O_2$ also occurs easily and oxidatively in a conventional photoelectrochemical system *i.e.* the redox potential of $H_2O_2$ degradation is more negative than the redox potential of $H_2O_2$ production from $H_2O$ (eqn (1) and (2)), resulting in low selectivity for oxidative $H_2O_2$ generation.

$$H_2O_2 \rightarrow O_2 + 2H^+ + 2e^- \ (E(O_2/H_2O_2) = +0.68 \text{ V } \textit{vs.} \text{ RHE}) \quad (2)$$

Recently, we reported that a photoelectrochemical system combining the $WO_3/BiVO_4$ photoanode and aqueous electrolyte of $KHCO_3$ under $CO_2$ bubbling could achieve simultaneous generation and accumulation of $H_2O_2$ and $H_2$ from $H_2O$ (eqn (3)).[28,29] In this system, the aqueous electrolyte of $KHCO_3$ acts as an excellent oxidative catalyst for generating $H_2O_2$ from $H_2O$. Moreover, $H_2O_2$ could be produced at no external bias on both a $WO_3/BiVO_4$ photoanode (from $H_2O$) and an Au cathode (from $O_2$) *via* a two-photon process (eqn (4)).[29]

$$2H_2O \rightarrow H_2O_2 + H_2 \text{ (two-photon process)} \quad (3)$$

$$2H_2O + O_2 \rightarrow 2H_2O_2 \text{ (two-photon process)} \quad (4)$$

Although the selectivity (faradaic efficiency: $\eta(H_2O_2)$) of reductive $H_2O_2$ production from $O_2$ on cathodes such as Au was very high, almost 100%, the maximum selectivity ($\eta(H_2O_2)$) for oxidative $H_2O_2$ production on $WO_3/BiVO_4$ photoanodes was still

[a]*Research Center for Photovoltaics (RCPV), National Institute of Advanced Industrial Science and Technology (AIST), Central 5, 1-1-1 Higashi, Tsukuba, Ibaraki 305-8565, Japan. E-mail: k.sayama@aist.go.jp*

[b]*Department of Pure and Applied Chemistry, Tokyo University of Science, 2641 Yamasaki, Noda, Chiba 278-8514, Japan*

† Electronic supplementary information (ESI) available: Experimental section, SEM images, XRD spectra, LHE spectra, applied voltage properties, *I–V* characteristic of photoanodes, pore size distribution of the $MeO_x$ particles, effect of $Al_2O_3$ amount on $WO_3/BiVO_4$ and dependence of applied voltage. See DOI: 10.1039/c7ra09693c

low, only *ca.* 54%. The design of novel photoanodes capable of achieving efficient $H_2O_2$ generation and inhibiting oxidative degradation of generated $H_2O_2$ is absolutely imperative for building a clean and breakthrough technology, by accumulating $H_2O_2$ and $H_2$ with unprecedented $H_2O_2$ selectivity using only $H_2O$ as the raw material.

Here, we focused on a surface modification of the metal oxide ($MeO_x$) layers on the $WO_3/BiVO_4$ photoanode surface to achieve excellent selectivity of generation and accumulation of $H_2O_2$ in the $KHCO_3$ aqueous solution under simulated solar light irradiation (Fig. 1). The $MeO_x$ layers were prepared by spin-coating of metal organic solutions and calcination. Introducing a porous $Al_2O_3$ layer was found to specifically permit oxidative $H_2O_2$ generation and accumulation with exceptional selectivity in an aqueous $KHCO_3$ electrolyte because of the blocking effect of oxidative degradation of the generated $H_2O_2$ into $O_2$ on the photoanode.

Details regarding experimental procedures for preparation and photoelectrochemical reactions of photoanodes are provided in the ESI†.

The effects of $MeO_x$ layers, modified on the $WO_3/BiVO_4$ photoanode, for oxidative $H_2O_2$ generation properties were investigated at an applied electric charge of 0.9C (900 s at steady photocurrent of 1 mA) in a 0.5 M $KHCO_3$ aqueous electrolyte. As shown in Fig. 2, all $MeO_x$-coated photoanodes, except $CoO_x$, enhanced the oxidative $H_2O_2$ generation compared to a bare $WO_3/BiVO_4$ photoanode, and the enhanced effect, ranked by the modified metal oxide, was $Al_2O_3 > ZrO_2 > TiO_2 > SiO_2 >> CoO_x$. Little $H_2O_2$ was observed on the $CoO_x$ coated photoanode, because $CoO_x$ probably decomposed the generated $H_2O_2$ quickly, or $O_2$ may be evolved on $CoO_x$ directly. It should be noted that the $Al_2O_3$ modification on the $WO_3/BiVO_4$ photoanode achieved roughly twice the oxidative $H_2O_2$ generation compared to the bare $WO_3/BiVO_4$ photoanode. The $Al_2O_3$ uniformly, smoothly and flatly covered the entire area of the $WO_3/BiVO_4$ photoanode as shown in the SEM images (Fig. 3), whereas other $MeO_x$ were granularly and uniformly supported on that and possessed any crack holes (Fig. S1; ESI†). It was also confirmed, from XRD measurement (Fig. S2; ESI†), that no

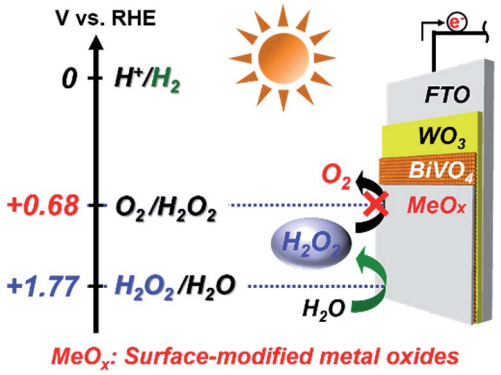


Fig. 1 Pattern and energy diagrams for photoelectrochemical $H_2O_2$ generation from $H_2O$ on $WO_3/BiVO_4/MeO_x$ photoanodes under solar light irradiation.

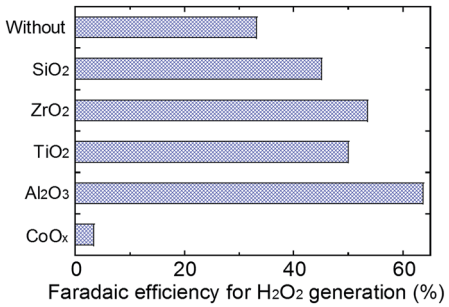


Fig. 2 Oxidative $H_2O_2$ generation on photoanodes ($WO_3/BiVO_4/MeO_x$) modified various metal oxides on a $WO_3/BiVO_4$ at an electric charge of 0.9C (900 s at steady photocurrent of 1 mA) in a 0.5 M $KHCO_3$ aqueous electrolyte (35 mL) in an ice bath (below 5 °C) under simulated solar light.

diffraction peaks derived from $MeO_x$ were observed in all $WO_3/BiVO_4/MeO_x$ photoanodes, suggesting that all tried $MeO_x$ modified on $WO_3/BiVO_4$ photoanode possess amorphous-like structure. As shown in Fig. S3; ESI,† little change of the light harvesting efficiency (LHE) was also confirmed in tried all photoanodes, suggesting that these $MeO_x$ introduced on the $WO_3/BiVO_4$ have little effect to light absorption efficiency on $WO_3/BiVO_4$ photoanode. The time courses of voltages applied between photoanode and a counter electrode of Pt mesh at steady photocurrent of 1 mA (Fig. 2) in oxidative $H_2O_2$ generation reaction were also confirmed (Fig. S4; ESI†). The voltages for applying steady photocurrent of 1 mA slightly increased by introducing $MeO_x$ on the $WO_3/BiVO_4$ photoanode. In particular, $WO_3/BiVO_4/Al_2O_3$ photoanode, coated uniformly, smoothly and flatly at $Al_2O_3$ compared to other $MeO_x$, required highest applied voltage. In order to confirm the effect introducing the $Al_2O_3$ on the photoanode in more detail, the photocurrent property of the $WO_3/BiVO_4/Al_2O_3$ photoanode was investigated in a 0.5 M $KHCO_3$ aqueous solution (Fig. S5; ESI†). The bare $WO_3/BiVO_4$ photoanode exhibited excellent photocurrent property in all applied voltage ranges as with our past reported example,[11,12,28,29] and the photocurrent property slightly decreased by introducing the $Al_2O_3$ layer. However, it should be noted that the decreasing degree of the photocurrent property was slight, only *ca.* 9% and 5% at +1.23 V and +1.77 V *vs.* RHE, respectively, although the $Al_2O_3$, having an insulation property, covered the entire area of the $WO_3/BiVO_4$ photoanode. A similar

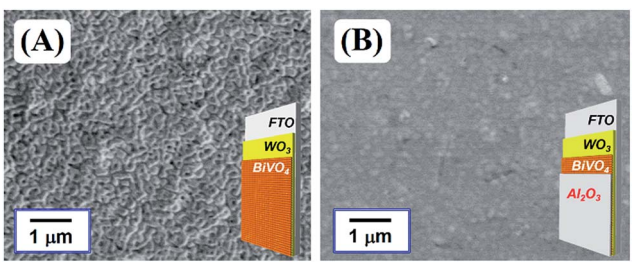


Fig. 3 SEM images of (A) $WO_3/BiVO_4$ and (B) $WO_3/BiVO_4/Al_2O_3$ photoanodes.

phenomenon has also been observed in $O_2$ and $H_2$ generation through water splitting on a photoanode coated with amorphous-like $Ta_2O_5$.[32] In addition, it was confirmed, from the $N_2$ absorption and desorption measurement of $MeO_x$ particles (Fig. S6; ESI†), that almost all $MeO_x$ possess mesoporous structure at a pore size of *ca.* 4–20 nm. In particular, a pore size of the $Al_2O_3$ was *ca.* 4.7 nm. The thicknesses of $Al_2O_3$ calculated from the coating amount on the $WO_3/BiVO_4$ photoanode by XRF measurement were *ca.* 100 nm (0.055 mg $cm^{-2}$). In order to also investigate the effects of dense $Al_2O_3$ on $WO_3/BiVO_4$ on the oxidative $H_2O_2$ generation, increasing $Al_2O_3$ amount on $WO_3/BiVO_4$ photoanode was performed by decreasing the spin coating number (500 rpm) of precursor solution of EMOD solved in butyl acetate containing ethylcellulose when introducing $Al_2O_3$ layers. The thickness of $Al_2O_3$ introduced at 500 rpm calculated from the XRF measurement was *ca.* 127 nm (0.070 mg $cm^{-2}$), suggested that the thickness increases with decreasing the spin coating number. As shown in Fig. S7; ESI,† little change of the $H_2O_2$ generation amounts was observed on these $WO_3/BiVO_4/Al_2O_3$ photoanodes prepared at 500 and 1000 rpm, indicating that increasing $Al_2O_3$ on $WO_3/BiVO_4$ photoanode has little effect on the oxidative $H_2O_2$ generation. In subsequent experiments, $WO_3/BiVO_4/Al_2O_3$ photoanode prepared at 1000 rpm was utilized as the photoanode. These results indicate that the specific effect enhancing oxidative $H_2O_2$ generation property was achieved on the $WO_3/BiVO_4$ though the mesoporous and amorphous $Al_2O_3$ layer covered uniformly, smoothly and flatly the entire area.

To track the specific performance enhancing effect of generating $H_2O_2$ by introducing the $Al_2O_3$ layer, the concentration dependency of $KHCO_3$ aqueous electrolytes on the oxidative $H_2O_2$ generation property was investigated at an applied electric charge of 0.9C (Fig. 4(A)). We have already reported that the oxidative $H_2O_2$ generation property on the $WO_3/BiVO_4$ photoanode was improved with increasing concentration of $KHCO_3$, which acts as an effective catalyst for $H_2O_2$ generation *via* the two-electron oxidation of $H_2O$.[28] Even in the case of using the $WO_3/BiVO_4/Al_2O_3$ photoanode, the selectivity ($\eta(H_2O_2)$) for $H_2O_2$ generation was significantly enhanced with increasing concentration of $KHCO_3$, and the $\eta(H_2O_2)$ in the 2.0 M $KHCO_3$ aqueous solution reached *ca.* 80% at 0.9C, whereas that using the bare $WO_3/BiVO_4$ photoanode was *ca.* 54%. It should be noted that the selectivity ($\eta(H_2O_2)$ = *ca.* 53%) on the $WO_3/BiVO_4/Al_2O_3$ photoanode in lowly concentrated $KHCO_3$ (0.1 M) was comparable to that (*ca.* 54%) on the bare $WO_3/BiVO_4$ photoanode in highly concentrated $KHCO_3$ (2.0 M). This suggests that the $Al_2O_3$ could effectively be contributing to oxidative $H_2O_2$ generation from $H_2O$ even in the lowly concentrated $KHCO_3$. Moreover, as shown in Fig. 4(B), the excellent $H_2O_2$ generation property on the $WO_3/BiVO_4/Al_2O_3$ photoanode compared to the $WO_3/BiVO_4$ photoanode was significantly maintained even at high electric charge up to 50C. As a result, the accumulation amount, using the $WO_3/BiVO_4/Al_2O_3$ photoanode, reached >2500 μM at 50C, while that using the bare $WO_3/BiVO_4$ photoanode was >1300 μM at 50C. The dependency of the applied voltage on the oxidative $H_2O_2$ generation was investigated to confirm the effect of the $Al_2O_3$ coating in detail (Fig. S8; ESI†). A small change in $H_2O_2$ generation performance was observed in all ranges of applied voltages (0.8–1.8 V), suggesting that the enhanced effect of introducing an $Al_2O_3$ layer is independent of the voltages applied between a photoanode as the working electrode and a Pt mesh as counter electrode using the aqueous electrolyte of the $KHCO_3$.

Although little development with regards to highly selective $H_2O_2$ generation *via* two-photon oxidation of $H_2O$ and accumulation using photoanodes has been reported, our method of $Al_2O_3$ coating on the $WO_3/BiVO_4$ photoanode produced tremendous improvement in selective $H_2O_2$ generation and accumulation from $H_2O$ in a $KHCO_3$ aqueous electrolyte. It is speculated that the specific enhancement of selectivity for $H_2O_2$ generation on the $WO_3/BiVO_4/Al_2O_3$ photoanode may be caused by a blocking effect, on the mesoporous $Al_2O_3$ layer, that inhibits oxidative $H_2O_2$ degradation into $O_2$ on the $BiVO_4$. To investigate the blocking effect on the $Al_2O_3$ layer, a degradation property test of $H_2O_2$ was performed in a 2.0 M $KHCO_3$ aqueous solution containing $H_2O_2$ (550 μM) in the presence of the bare $WO_3/BiVO_4$ or $WO_3/BiVO_4/Al_2O_3$ photoanodes in presence or absence of simulated solar light irradiation in an ice bath (below 5 °C). In both cases, as shown in Fig. 5, almost all the initial amount of $H_2O_2$ was maintained in the dark condition, however, the $H_2O_2$ amount drastically decreased with irradiation by simulated solar light, suggesting that the $H_2O_2$ was decomposed by photocarriers (excited electrons and holes) produced on the $BiVO_4$. It should be noted that the $H_2O_2$ degradation in the presence of the $WO_3/BiVO_4/Al_2O_3$ photoanode was dramatically inhibited compared to the degradation in the presence of a bare $WO_3/BiVO_4$ photoanode. The oxidative $H_2O_2$ generation test was also confirmed in a 2.0 M $KHCO_3$ aqueous electrolyte, initially containing $H_2O_2$ (210 μM) on the bare $WO_3/BiVO_4$ and $WO_3/BiVO_4/Al_2O_3$ photoanodes, to track the generated $H_2O_2$ degradation behaviour in more detail (Fig. 6). The generated rates of $H_2O_2$ were reduced by the initial addition of $H_2O_2$ in both cases of presence or absence of $Al_2O_3$.

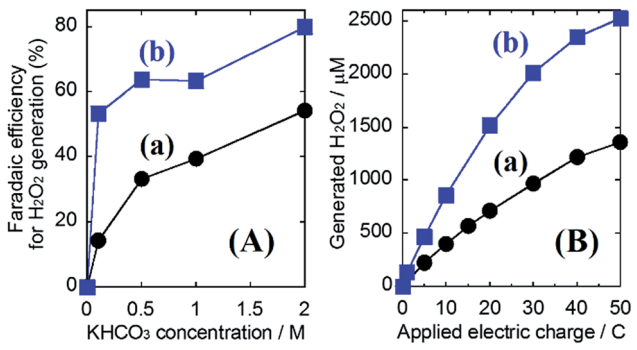


Fig. 4 (A) Oxidative $H_2O_2$ generation in $KHCO_3$ aqueous electrolytes (35 mL) of different concentrations at applied electric charges of 0.9C (900 s at steady photocurrent of 1 mA) under simulated solar light and (B) accumulation of oxidative $H_2O_2$ generation in a 2.0 M $KHCO_3$ aqueous solution (35 mL) under visible light irradiation ($\lambda$ > 420 nm) using an intense Xe lamp at an applied voltage of 1.5 V in an ice bath (below 5 °C) on a (a) bare $WO_3/BiVO_4$ and (b) $WO_3/BiVO_4/Al_2O_3$ photoanodes.

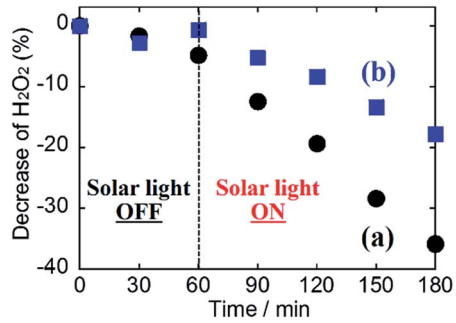


Fig. 5 Degradation properties of $H_2O_2$ (550 μM) initially added in a 2.0 M $KHCO_3$ aqueous solution in an ice bath (below 5 °C) under $CO_2$ bubbling and simulated solar light irradiation in the presence of a (a) $WO_3/BiVO_4$ and (b) $WO_3/BiVO_4/Al_2O_3$ photoanodes at no applied voltage.

However, the decreasing rate of $H_2O_2$ generation was significantly inhibited, from *ca.* 61% to *ca.* 39%, by introducing the $Al_2O_3$ layer on the $WO_3/BiVO_4$ photoanode. These results suggest that introducing the $Al_2O_3$ layer significantly contributed to the highly selective $H_2O_2$ generation and accumulation from $H_2O$, with a high photocurrent property, by a blocking effect that inhibited the oxidative degradation of generated $H_2O_2$. The mechanism of blocking effect is proposed that the $H_2O_2$ generated on the $BiVO_4$ in the $WO_3/BiVO_4/Al_2O_3$ photoanode diffuses in electrolyte of $KHCO_3$ aqueous solution through mesoporous of the $Al_2O_3$, and contact of the $H_2O_2$ diffused in electrolyte with the $BiVO_4$ covered uniformly and smoothly $Al_2O_3$ may be significantly inhibited compared with that with bare $BiVO_4$, resulting in the formation of effective inhibition of oxidative $H_2O_2$ degradation. Furthermore, there may be other possible mechanisms such as a blocking effect of a direct $O_2$ evolution site *via* a 4-photon process covering by $Al_2O_3$, or an enrichment effect resulting from the increasing $KHCO_3$ concentration around the photoanode based on the acid–base adsorption between $HCO_3^-$ (a weak base) and the weakly acidic sites on the $Al_2O_3$ surface, related to the good

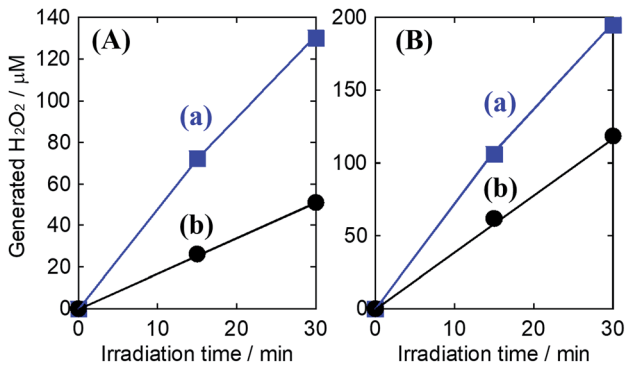


Fig. 6 Comparison of oxidative $H_2O_2$ generation in a 2.0 M $KHCO_3$ aqueous electrolyte (a) in the absence of or (b) containing initially-added $H_2O_2$ (210 μM) in an ice bath (below 5 °C) on a (A) $WO_3/BiVO_4$ and (B) $WO_3/BiVO_4/Al_2O_3$ photoanodes under simulated solar light irradiation at steady photocurrent of 1 mA.

$\eta(H_2O_2)$ in lower $KHCO_3$ concentration, as shown in Fig. 4(A). The tracking and contribution of these other mechanisms, on the $Al_2O_3$ layer, is currently under investigation.

## Conclusions

In summary, various metal oxides were coated onto a $WO_3/BiVO_4$ photoanode to enhance the selectivity (faradaic efficiency) of oxidative $H_2O_2$ generation, in an aqueous electrolyte of $KHCO_3$, from water under solar light irradiation. Among the various metal oxides, the $Al_2O_3$ coating, which produced a mesoporous and amorphous structure on the $WO_3/BiVO_4$ photoanode, achieved excellent oxidative $H_2O_2$ generation at a selectivity of *ca.* 80% and an accumulation of >2500 μM (50C). Interestingly, the $Al_2O_3$-coated $WO_3/BiVO_4$ photoanode dramatically inhibited oxidative degradation of $H_2O_2$ generated on the $WO_3/BiVO_4$ photoanode after introducing the $Al_2O_3$ layer. This study contributes to developing a promising design for a clean $H_2O_2$ production system that uses only water as the raw material under solar light irradiation. More effective dreamy $H_2O_2$ generation, at an excellent selectivity close to 100%, can be expected by modifying the surface-treatment technology, and it is currently under investigation.

## Conflicts of interest

There are no conflicts to declare.

## Acknowledgements

The present work was partially supported by JSPS KAKENHI Grant Number 26810105 and the International Joint Research Program for Innovative Energy Technology. We thank Dr Etsuko Fujita (Brookhaven National Laboratory) for helpful discussions.

## Notes and references

1 A. Fujishima and K. Honda, *Nature*, 1972, **238**, 37.
2 Z. G. Zou, J. H. Ye, K. Sayama and H. Arakawa, *Nature*, 2001, **414**, 625.
3 A. Kudo and Y. Miseki, *Chem. Soc. Rev.*, 2009, **38**, 253.
4 K. Maeda, K. Teramura, D. Lu, T. Takata, N. Saito, Y. Inoue and K. Domen, *Nature*, 2006, **440**, 295.
5 K. Fuku, K. Hashimoto and H. Kominami, *Chem. Commun.*, 2010, **46**, 5118.
6 K. Fuku, T. Kamegawa, K. Mori and H. Yamashita, *Chem.–Asian J.*, 2012, **7**, 1366.
7 K. Fuku, R. Hayashi, S. Takakura, T. Kamegawa, K. Mori and H. Yamashita, *Angew. Chem., Int. Ed.*, 2013, **52**, 7446.
8 B. D. Alexander, P. J. Kulesza, I. Rutkowska, R. Solarska and J. Augustynski, *J. Mater. Chem.*, 2008, **18**, 2298.
9 K. Sayama, A. Nomura, Z. Zou, R. Abe, Y. Abe and H. Arakawa, *Chem. Commun.*, 2003, 2908.
10 P. Chatchai, Y. Murakami, S. Kishioka, A. Y. Nosaka and Y. Nosaka, *Electrochim. Acta*, 2009, **54**, 1147.

11 R. Saito, Y. Miseki and K. Sayama, *Chem. Commun.*, 2012, **48**, 3833.
12 I. Fujimoto, N. Wang, R. Saito, Y. Miseki, T. Gunji and K. Sayama, *Int. J. Hydrogen Energy*, 2014, **39**, 2454.
13 X. Shi, I. Y. Choi, K. Zhang, J. Kwon, D. Y. Kim, J. K. Lee, S. H. Oh, J. K. Kim and J. H. Park, *Nat. Commun.*, 2014, **5**, 4775.
14 T. W. Kim and K. S. Choi, *Science*, 2014, **343**, 990.
15 Y. Liu, Y. Guo, L. T. Schelhas, M. Li and J. W. Ager III, *J. Phys. Chem. C*, 2016, **120**, 23449.
16 L. H. Hess, J. K. Cooper, A. Loiudice, C. M. Jiang, R. Buonsanti and I. D. Sharp, *Nano Energy*, 2017, **34**, 375.
17 J. Su, L. Guo, N. Bao and C. A. Grimes, *Nano Lett.*, 2011, **11**, 1928.
18 P. M. Rao, L. Cai, C. Liu, I. S. Cho, C. H. Lee, J. M. Weisse, P. Yang and X. Zheng, *Nano Lett.*, 2014, **14**, 1099.
19 I. Grigioni, K. G. Stamplecoskie, D. H. Jara, M. V. Dozzi, A. Oriana, G. Cerullo, P. V. Kamat and E. Selli, *ACS Energy Lett.*, 2017, **2**, 1362.
20 K. Mase, M. Yoneda, Y. Yamada and S. Fukuzumi, *ACS Energy Lett.*, 2016, **1**, 913.
21 F. M. Toma, J. K. Cooper, V. Kunzelmann, M. T. McDowell, J. Yu, D. M. Larson, N. J. Borys, C. Abelyan, J. W. Beeman, K. M. Yu, J. Yang, L. Chen, M. R. Shaner, J. Spurgeon, F. A. Houle, K. A. Persson and I. D. Sharp, *Nat. Commun.*, 2016, **7**, 12012.
22 J. Y. Kim, G. Magesh, D. H. Youn, J. W. Jang, J. Kubota, K. Domen and J. S. Lee, *Sci. Rep.*, 2013, **3**, 2681.
23 Q. Mi, A. Zhanaidarova, B. S. Brunschwig, H. B. Gray and N. S. Lewis, *Energy Environ. Sci.*, 2012, **5**, 5694.
24 J. C. Hill and K. S. Choi, *J. Phys. Chem. C*, 2012, **116**, 7612.
25 K. Ueno and H. Misawa, *NPG Asia Mater.*, 2013, **5**, e61.
26 K. Fuku, N. Wang, Y. Miseki, T. Funaki and K. Sayama, *ChemSusChem*, 2015, **8**, 1593.
27 H. G. Cha and K. S. Choi, *Nat. Chem.*, 2015, **7**, 328.
28 K. Fuku and K. Sayama, *Chem. Commun.*, 2016, **52**, 5406.
29 K. Fuku, Y. Miyase, Y. Miseki, T. Funaki, T. Gunji and K. Sayama, *Chem.–Asian J.*, 2017, **12**, 1111.
30 K. Fuku, Y. Miyase, Y. Miseki, T. Gunji and K. Sayama, *ChemistrySelect*, 2016, **1**, 5721.
31 T. Shiragami, H. Nakamura, J. Matsumoto, M. Yasuda, Y. Suzuri, H. Tachibana and H. Inoue, *J. Photochem. Photobiol., A*, 2015, **313**, 131.
32 R. Saito, Y. Miseki, W. Nini and K. Sayama, *ACS Comb. Sci.*, 2015, **17**, 592.